Phytochrome-imposed inhibition of PIF7 activity shapes photoperiodic growth in Arabidopsis together with PIF1, 3, 4 and 5

Pablo Leivar[1,2,a,b], Guiomar Martín[1], Judit Soy[1], Jutta Dalton-Roesler[3], Peter H. Quail[3], and Elena Monte[1,a,b]

[1] Department of Molecular Genetics, Centre for Research in Agricultural Genomics (CRAG) CSIC-IRTA-UAB-UB. Campus UAB, Bellaterra, Barcelona, Spain.

[2] Laboratory of Biochemistry, Institut Químic de Sarrià, Universitat Ramon Llull. Barcelona, Spain.

[3] Department of Plant and Microbial Biology, University of California-Berkeley, and United States Department of Agriculture, Plant Gene Expression Center, USA.

[a] Equal contribution.

[b] To whom correspondence should be addressed. E-mail: pablo.leivar@iqs.url.edu, elena.monte@cragenomica.es.

Running Title:

PIF7 and PIFq regulation of photoperiodic growth

ABSTRACT

Under photoperiodic conditions, *Arabidopsis thaliana* seedling growth is inhibited in long days (LD), but promoted under the extended nights of short days (SD). This behavior is partly implemented by phytochrome (phy)-imposed oscillations in the abundance of the growth-promoting, phy-interacting bHLH transcription factors PHY-INTERACTING FACTOR 1 (PIF1), PIF3, PIF4 and PIF5 (PIF quartet or PIFq). However, the observation that a *pifq* mutant is still stimulated to elongate when given a phy-inactivating end-of-day far-red pulse (EODFR), suggests that additional factors are involved in the phy-mediated suppression of growth during the subsequent dark period. Here, by combining growth-analysis of *pif7* single- and higher-order mutants with gene expression analysis under SD, LD, SD-EODFR, and LD-EODFR, we show that PIF7 promotes growth during the dark hours of SD, by regulating growth-related gene expression. Interestingly, the relative contribution of PIF7 in promoting growth is stronger under EOD-FR, while PIF3 role is more important under SD, suggesting that PIF7 is a prominent target of phy-suppression. Indeed, we show that in SD, phy imposes phosphorylation and inactivation of PIF7 during the light hours, and prevents full dephosphorylation during the night. This repression can be lifted with an EODFR, which correlates with increased PIF7-mediated gene expression and elongation. In addition, our results suggest that PIF7 function might involve heterodimerization with PIF3. Furthermore, our data indicate that a *pifqpif7* quintuple mutant is largely insensitive to photoperiod for hypocotyl elongation. Collectively, the data suggest that PIF7, together with the PIFq, are required for the photoperiodic regulation of seasonal growth.

Abbreviations:

EOD-FR, end-of-day far red; FRp, far red pulse; LD, long day; PHY, phytochrome; PIF, phy-interacting factor; PIF7; SD, short day.

INTRODUCTION

Phytochrome interacting factors (PIFs) are basic helix-loop-helix transcriptional regulators that are promoters of elongation growth in *Arabidopsis thaliana* (Leivar and Monte 2014). PIFs interact specifically with the active Pfr conformer of phytochrome (phy) photoreceptors. In the dark, the phy inactive red (R) light-absorbing Pr conformer is localized in the cytosol and PIFs accumulate in the nucleus. Upon light exposure, phy Pr converts to the biologically active far red (FR) light-absorbing Pfr form, which translocates into the nucleus and interacts with the PIFs, triggering rapid degradation of the PIF quartet (PIFq) members PIF1, PIF3, PIF4 and PIF5 (with half-lives of 5-20 min) (Pham et al. 2018). Of the five phytochromes in Arabidopsis (phyA-phyE), phyA and phyB dominate the regulation of PIF degradation (Bauer et al. 2004, Al-Sady et al. 2006, Shen et al. 2007, 2008). Importantly, thanks to the reversible photoconversion between the Pr and the Pfr phy conformers (Al-Sady et al. 2006, Shen et al. 2007, 2008), PIF levels oscillate in environments with fluctuations in Pr and Pfr levels such as under low Red (R)/Far Red (FR) ratio conditions typical of shade environments, or in diurnal light-dark cycles.

Under short-day (SD) photoperiods, growth is rhythmic with maximal hypocotyl elongation rates at the end of the night (Nozue et al. 2007), largely due to the combined actions of the PIFq, which accumulate during the night and promote growth at dawn (Nozue et al. 2007, Niwa et al. 2009, Soy et al. 2012, 2014). Transition to the morning light destabilizes the PIFs and growth rate is rapidly reduced again (Nozue et al. 2007, Soy et al. 2012). Specific dawn-phased PIF accumulation and activity in SD is regulated at several levels (Gommers and Monte 2018). First, photoactivated Pfr imposes a decrease in PIFq proteins during the day and early night, whereas slow progressive Pfr-to-Pr reversion in the dark allows reaccumulation of these PIFs towards the end of the night (Monte et al. 2004, Shen et al. 2005, Nozue et al. 2007, Soy et al. 2012, Yamashino et al. 2013). Second, *PIF4* and *PIF5* expression is regulated by the circadian clock, and their transcripts oscillate to peak at dawn, superimposed on the control of their protein stabilization by light (Nozue et al. 2007, Nusinow et al. 2011, Yamashino et al. 2013). In contrast, *PIF1* and *PIF3* transcript levels are relatively constant. Moreover, the capacity of PIFs to bind DNA is inhibited by photoactive phyB (Park et al. 2018) and gibberellins/DELLAs (Arana et al. 2011). Finally, PIF activity is regulated by circadian clock components like PRRs, ELF3 or GIGANTEA (Soy et al. 2016, Martín et al. 2018, Nieto et al. 2015, Zhang et al. 2020, Nohales et al. 2019), or by the brassinosteroid pathway (Oh et al. 2012, Bernardo-García et al. 2014).

Of the PIFq proteins, PIF3 appears to play a more prominent role under SD (Soy et al. 2014). Growth promotion by PIF3 and the rest of the PIFq proteins involves direct induction of the growth-related genes *PIL1*, *XTR7* and *HFR1* (Hornitschek et al. 2009, Soy et al. 2012, Leivar et al. 2012b), as well as regulation of auxin- and other hormone-related genes (Nozue et al. 2011, Nomoto et al. 2012). Importantly, the observation that *pifq* mutants still retained elongation

responses after a phy-inactivating end-of-day (EOD) FR pulse suggests redundancy with additional PIFs (Leivar et al. 2012a, 2012b, Soy et al. 2014).

In contrast to PIFq, PIF7 protein is relatively light stable (Leivar et al. 2008a, Li et al. 2012), and phy mediates the accumulation of a phosphorylated form of PIF7 in high R/FR. This phosphorylated form of PIF7 is retained in the cytosol by 14-3-3 proteins (Huang et al. 2018) and is thus unable to bind to its target genes (Li et al. 2012). Under the low R/FR conditions of shade, where PIF7 appears to play a major role (Li et al. 2012, de Wit et al. 2015, 2016), inactivation of phy promotes nuclear accumulation of dephosphorylated PIF7 that is able to bind and induce the expression of target genes in part by recruiting chromatin remodeling machinery (Li et al. 2012, Peng et al. 2018). PIF7 is also involved in shade-induced flowering (Galvão et al. 2019, Zhang et al. 2019). In contrast to shade, the role of PIF7 under photoperiodic growth conditions remains poorly understood.

Here, by genetic analysis of *pif7* mutants, we show that PIF7 is a prominent target of phyB-mediated suppression of growth at night, when it promotes growth in SD and especially under SD-EODFR conditions. In order to assess the relative contributions of PIFq members and PIF7, we examine the response of multiple *pif* mutants under different photoperiods and report that the *pifqpif7* quintuple mutant, lacking five PIFs (PIF1, 3, 4, 5 and 7), is largely insensitive to the phy-mediated seasonal control of growth. Moreover, we show functional interactions between PIF7 and PIF3 that might involve PIF7-PIF3 heterodimers. Finally, we examine how PIF7 is regulated during the diurnal cycle at the transcriptional and protein level.

MATERIALS AND METHODS

Plant materials

Some of the mutant lines used in this study were described elsewhere including PIF7-FLASH (Li et al. 2012), *phyB-9* (Reed et al. 1993), *pif3-3* (Monte et al. 2004), *pif7-1*, *pif3pif7*, *phyBpif7* and *pif3pif4* (Leivar et al. 2008a), and *pif3pif4pif5* and *pif1pif3pif4pif5* (*pifq*) (Leivar et al. 2008b). New mutant combinations included *pif3pif4pif7*, which was generated by crossing *pif3pif4* and *pif3pif7*, and *pif3pif4pif5pif7* and the quintuple *pifqpif7* mutant (Zhang et al. 2020), which were generated by crossing *pif3pif4pif7* and *pifq*.

Seedling growth and Measurements

Upon sterilization, seeds were plated in GM medium without sucrose and stratified for four days in darkness (D) at 4ºC as described (Monte et al. 2003, Soy et al. 2014). Plates were then transferred to either constant white light (WL, 85 μmol/m^{2}s), long-days (LDs, 16hWL:8hD) or short-days (SDs, 8hWL:16hD), or to LDs or SDs submitted to a 15min saturating FR pulse (30 μmol/m^{2}s) at the end of the day period (LD-EODFR and SD-EODFR) before the night hours.

Seedlings were arranged horizontally on a plate and photographed using a digital camera (Nikon D80) as described (Soy et al. 2014). Hypocotyl elongation was measured typically from at least

25 seedlings using NIH Image software (ImageJ, National Institutes of Health). Differences between means were statistically analyzed by one-way analysis of variance using Tukey multiple comparison test (GraphPad Prism6). Statistically significant differences were defined as those with a p value < 0.05.

In vitro Co-immunoprecipitaton assay

In vitro coimmunoprecipitation experiments were essentially as described (Khanna et al. 2004). Briefly, each protein was expressed from T7 promoters using the TnT in vitro transcription/translation system (Promega). PIF7:GAD and GAD:PIF3 constructs were described previously (Leivar et al. 2008a, Ni et al. 1998), whereas naked PIF7 corresponds to the full-length open reading frame cloned into the pET17b vector using SacI and XhoI sites (Invitrogen, CA). Proteins in each binding reaction were cosynthesized as ^{35}S-Met-labeled products in TnT reactions as specified. Signals were quantified with a Storm 860 PhosphorImager (Molecular Dynamics).

Yeast-two hybrid assay

GAD alone or fused to full length PIF3 (GAD:PIF3) in pGAD424 (Ni et al. 1998) and GAL4 DNA Binding domain (GBD) alone or fused to full length PIF7 (GBD:PIF7) in pGBKT7 were used for yeast two-hybrid interaction assays in yeast strains AH109 and Y187 following the Clontech (Palo Alto, CA) Yeast Protocol Handbook.

Electrophoresis mobility shift assay (EMSA)

Electromobility shift assays were performed as described (Martínez-García et al. 2000), but with pLUC control plasmid added to the binding reactions (Toledo-Ortiz et al. 2003). All proteins were expressed from T7 promoters using the TnT in vitro transcription/translation system (Promega). Naked PIF3 (Fairchild et al. 2000) and GAD:PIF3 (Ni et al. 1999) constructs were described elsewhere, and naked PIF7 is described above. PIF7 and GAD:PIF3 were synthesized separately (Fig. 3, lanes 4 and 3 respectively) or cosynthesized (Fig. 3 lane 5) in TnT reactions, and 3µL of these TnT mixes were used for DNA binding. A total of 30,000 cpm of labeled G-box probe was used in each lane. The binding conditions were as described (Leivar et al. 2008a).

Gene expression analysis

For gene expression, RNA extraction, cDNA synthesis and qRT-PCR were performed as described (Sentandreu et al. 2011, Soy et al. 2012, 2014). In the time-course analysis performed here, the gene expression was measured from three technical replicates for each time point and genotype. *PP2A* (*AT1G13320*) was used as a normalization control as described (Shin et al. 2007, Leivar et al. 2009). Primers for the gene expression analysis of *PIL1* (*AT2G46970*), *XTR7* (*AT4G14130*)**,** *HAT2* (*AT5G47370*), *MIDA9* (*AT5G02760*) and *HFR1* (*AT1G02340*) were described elsewhere (Soy et al. 2012, 2016, Sentandreu et al. 2011). *PIF7* (*AT5G61270*) expression was measured using primers EMP538 (5'-GTTTCAGATGTCGTTGCTTGCA-3') and EMP539 (5'-TACCCATAGGAGGGACCATCAT-3').

Protein Extraction and Immunoblots

Total protein extracts were obtained by resuspending grinded tissue samples in extraction buffer. Extraction buffer and protein quantification were done as described (Leivar et al. 2008a, Soy et al. 2016). PIF7-FLASH protein (Li et al. 2012) was detected after separation in a 7.5% SDS-PAGE gel, and immunodetection was performed using mouse monoclonal anti-cMYC (SIGMA). Peroxidase-linked anti-mouse antibody (Amersham Biosciences) were used as secondary antibodies to detect the MYC epitope. Images were captured using a LAS4000 system.

Accession numbers

Arabidopsis Genome Initiative database accession numbers are: AT2G20180 (PIF1/PIL5), AT1G09530 (PIF3), AT2G43010 (PIF4), AT3G59060 (PIF5/PIL6), AT5G61270 (PIF7), AT2G18790 (phyB).

RESULTS

phyB suppresses diurnal growth by antagonizing PIF7

Analyses of hypocotyl length in *Arabidopsis thaliana* wild-type (WT) and *pif7* mutant (Leivar et al. 2008a) seedlings grown for 4 days in short days (SDs) or in constant white light (WL) (Fig. 1A and 1B), showed that the enhanced elongation in SD compared to WL previously reported (Soy et al. 2012) depends on PIF7, since *pif7* hypocotyls were clearly shorter than WT in SDs but only marginally shorter in WL (Fig. 1B and 1C). In the *phyB* mutant background, *pif7* mutation partly suppressed the *phyB* elongated phenotype in both WL and SD (Fig. 1B and 1C). Particularly in SD, quantification showed that the *pif7* mutation in *phyBpif7* mutants suppressed a significant part of the striking SD-induced elongated phenotype of *phyB* mutants (3.1 mm vs 3.9 mm) compared to WT (1.1 mm) (Fig. 1D). Together, these results are consistent with an antagonistic interplay between phyB and PIF7 in regulating growth under photoperiodic conditions, similar to what was reported for PIF3 and other PIFq members (Soy et al. 2012, 2014), and suggest that phyB suppression of growth in response to the long nights of SDs occurs partly by inhibiting PIF7.

Analyses of photoperiodic conditions (SD and LD) supplemented with or without a 15-min phy-inactivating FR-pulse (FRp) at the end of the day (end-of-day-far red (EODFR)) (Fig. 1A) revealed that the *pif7* mutant displayed a short-hypocotyl phenotype only when the conditions included extended periods under inactive phy Pr conditions, such as SD, LD-EODFR and SD-EODFR (Fig. 1C, 1D). These data are consistent with recent reports that PIF7 induces growth under long-term low R/FR (Li et al. 2012) or in response to prolonged (2-3h) low R/FR exposure at EODFR under diurnal conditions (Mizuno et al. 2015, Jiang et al. 2019). However, in contrast to these reports where the elongation phenotype is mainly dependent on PIF7 (Mizuno et al. 2015, Jiang et al. 2019), in our brief saturating FRp-promoted EOD-FRp in SD schedule, the *pif7* mutant still retained significant growth responses, indicating that other PIF members likely contribute to

growth in our SD-EOD-FR conditions. Consistent with phyB being the major photoreceptor in perceiving the EODFR signal, the elongated hypocotyl phenotype of *phyB* was strongly attenuated in response to EODFR, especially under SD-EODFR conditions (Fig. 1C, 1D). In all the conditions tested, we observed that the *pif7* mutation partly suppressed the *phyB* mutant phenotype in a quantitatively similar manner (Fig. 1C, 1D), consistent with the view that PIF7 is a target of phyB in suppressing growth in WL and under photoperiodic conditions.

Photoperiodic control of growth is explained by the collective action of five PIFs

PIF1, PIF3, PIF4, and PIF5 have previously been reported to play a role in promoting growth under diurnal and EODFR conditions, with PIF3 being the main contributor to SD growth (Leivar et al. 2012a, 2012b, Soy et al. 2014, Nozue et al. 2007, Niwa et al. 2009). To assess the function of PIF7 in promoting photoperiodic growth, we first compared *pif3*, *pif7*, and *pif3pif7* mutants (Monte et al. 2004, Leivar et al. 2008a) under the photoperiodic conditions detailed in Fig. 1A, including EODFR treatments (Fig. 2A and 2B). Interestingly, while *pif3* was shorter than *pif7* under SD, *pif7* was clearly shorter than *pif3* under SD- and LD-EODFR, conditions where *pif3pif7* showed additive to synergistic effects (Fig. 2A, 2B, and 2C). Next, to investigate the role of PIF7 in the absence of multiple PIFq members, we generated a series of higher order *pif* mutants lacking PIF7 such *as pif3pif4pif7* and *pif3pif4pif5pif7*, and the quintuple mutant *pifqpif7* that lacked all five PIFs. The hypocotyl elongation of these mutants and the corresponding controls (namely *pif3pif4*, *pif3pif4pif7*, *pif3pif4pif5*, *pif3pif4pif5pif7*, *pifq*, *pifqpif7*) was examined under WL, LD, SD, or SD/LD-EODFR (Fig. 1A). Our results showed that they were: (1) only marginally shorter than WT in WL and LD (Fig. 2B and 2D); (2) shorter than WT under the long night of SDs, with no significant growth response compared to WL or LDs (Fig. 2C) and no additive effects as all the higher order *pif* mutants were similarly short in SDs (Fig. 2B and 2C); (3) shorter than WT under LD-EODFR conditions, with a marginal growth response in *pif3pif4*, *pif3pif4pif5*, and *pifq* mutants that was largely suppressed by the genetic removal of PIF7 in *pif3pif4pif7* mutants, *pif3pif4pif5pif7*, and *pifqpif7* mutants (Fig. 2B and 2C). Finally, under SD-EODFR (Fig. 1A), the strong growth of WT seedlings was attenuated to varying degrees in all higher order *pif* mutants (Fig. 2B and 2D), suggesting collective participation of all PIFs under these conditions. Interestingly, all higher order *pif* mutants carrying WT PIF7 (*pif3pif4*, *pif3pif4pif5*, and *pifq*) showed a limited but still significant growth response (Fig. 2B and 2C). Genetic removal of PIF7 further reduced the growth response (Fig. 2B and 2C), although *pif3pif4pif7* and *pif3pif4pif5pif7* still exhibited a residual growth response to the EODFR treatment indicating that the remaining PIFs (PIF1 or PIF5) are still active. Strikingly, the quintuple *pifqpif7* mutant was almost completely insensitive to the EODFR treatment (Fig. 2B and 2C). Together, these data indicate that the relative contribution of PIF7 to diurnal hypocotyl elongation is enhanced by phy

inactivation, and that the collective action of PIF1, 3, 4, 5, and 7 is sufficient to explain the photoperiodic regulation of seasonal growth.

PIF7 can form heterodimers with PIF3 that bind to DNA in vitro

PIF7 has been shown to form heterodimers with PIF1 and PIF4 in vitro (Castillon et al. 2007, Kidokoro et al. 2009, Fiorucci et al. 2019, Toledo-ortiz et al. 2003, Bu et al. 2011). To further assess the inter-PIF7 heterodimerization landscape, and given the prominent role of PIF3 in the regulation of growth under diurnal conditions (Soy et al. 2012, 2014) and the observed synergistic contributions of PIF3 and PIF7 to hypocotyl elongation (Fig. 2), we tested possible PIF7-PIF3 heterodimerzation. Indeed, *in vitro* pull-down assays confirmed direct interaction between PIF7 and PIF3 (Fig. 3A) that was confirmed in yeast two-hybrid *in vivo* assays (Fig. 3B). PIF7 was also shown to form homodimers *in vitro* (Fig. 3A), consistent with previous reports (Kidokoro et al. 2009, Fiorucci et al. 2019). Furthermore, using EMSA assays, we detected binding of PIF7 to G-box DNA elements as homodimer and as a PIF7-PIF3 heterodimer (Fig 3C). These results indicate that *in vitro*, PIF7 can heterodimerize with PIF3 and that this dimeric PIF7-PIF3 can bind to DNA, suggesting that functional interaction between PIF7 and PIF3 might involve heterodimer formation.

Contrasting developmental and temporal growth-promoting activities of PIF3 and PIF7 in SD and SD-EODFR.

To further understand the interplay between PIF3 and PIF7 along early growth in SD and SD-EODFR, we performed time-course phenotypic analysis at days 2, 3 and 4 (in contrast to the end-point measurements in 4d-old seedlings shown in Fig. 2). Under SDs, we observed that the short hypocotyl phenotype of *pif3* mutants was already established at day 2 (Fig. 4A) and maintained throughout the rest of the treatment, in agreement with previous data (Soy et al. 2012), whereas the short hypocotyl phenotype of *pif7* mutants was not manifested until day 4. In contrast, under SD-EODFR, the additive contributions of PIF3 and PIF7 were clearly observed by day 2 and throughout days 3 and 4 (Fig. 4A). Because some of the phenotypes are observed as early as 2 days, one possibility is that the participation of PIF3 is exclusively determined during early deetiolation. To test this possibility, we modified the experimental set up so that seedlings were first deetiolated for 2 days in WL, and then were kept for 4 additional days in either WL, SD or SD-EODFR. As shown in Fig. 4B, the observed phenotypes were roughly similar to Fig. 2: (1) WT hypocotyl induction in response to SD and SD-EODFR; (2) A more prominent short hypocotyl phenotype of *pif3* mutants in SD compared to *pif7*; (3) A more prominent short hypocotyl phenotype of *pif7* mutants in SD-EODFR compared to *pif3*; and (4) Additive effects observed in *pif3pif7* double mutants, in this case in both SD and SD-EODFR. These data suggest that the interplay between PIF3 and PIF7 under the tested photoperiodic conditions is not exclusively established early during early deetiolation, and instead is sustained in green seedlings.

The experiments presented above suggest that, similar to what has been reported for PIF3 and other PIFq members (Soy et al. 2012, 2014, Nozue et al. 2007, Monte et al. 2004, Shen et al. 2005), PIF7 acts to induce growth during the dark hours under diurnal conditions after phy repression is lifted. In order to test this possibility, we performed phenotypic measurements during the night period under SD conditions. First, *pif3* and *pif7* single and double mutants were grown for 2 days in SD, and during the 3rd day in SD the hypocotyl elongation was measured: (1) at ZT8, the end of the light period (W8); and (2) at the end of the night period (ZT24) in samples that had been (FR24) or not (D24) treated with an EODFR (Fig. 4C, left panel). Consistent with Fig. 4A, WT seedlings grew over the dark period (D24) of the 3rd day in SD in a strong PIF3-dependent manner with marginal to null contributions of PIF7 (Fig. 4C, middle and right panels), whereas EODFR-induced growth (FR24) was additively dependent on both PIF3 and PIF7.

PIF7, together with PIF3, acts to induce growth-related gene expression during the dark hours in SDs

In order to determine the interplay between PIF3 and PIF7 in regulating gene expression during the night period, we performed time-course experiments of *pif3* and *pif7* mutants grown in SD and in SD-EODFR following the same experimental design of Fig. 4C. In these experiments, samples were taken at the end of the light period of the 3rd day in SDs (ZT8; W8), and during the night in samples that had (FR) or not (D) been treated with an EODFR at ZT9 (D9, FR9), ZT12 (D12, FR12), ZT16 (D16, FR16), ZT20 (D20, FR20), and ZT24 (D24, W24). We also included a time point upon 1h illumination (ZT1, W25) at the 4th day in SDs. Initially we measured the expression of *PIL1*, *HFR1* and *XTR7*, genes that are directly induced by PIF3 during the night period in SDs (Soy et al. 2012), and in the case of *PIL1* and *HFR1*, they have also been shown to be regulated by PIF7 in response to shade (Li et al. 2012). The data show that under SDs, there is a progressive accumulation of *PIL1*, *HFR1*, and *XTR7* transcripts during the night in WT seedlings (Fig. 5A), which is strongly attenuated in *pif3* mutants as reported (Soy et al. 2012). *pif7* mutants also had reduced expression compared to WT, although it was not as strong and was more evident towards the end of the night (D24). Additive effects in *pif3pif7* double mutants were only marginally observed for *HFR1* (Fig. 5A). In sharp contrast, an EODFR treatment rapidly induced the expression of these genes in WT seedlings to expression values similar or even higher to those at the end of the night in SDs (D24, indicated as a horizontal dotted line) (Fig. 5B). The relative contribution of PIF3 and PIF7 in promoting early EODFR-induced gene expression varied in each case. For *PIL1*, a minor contribution of PIF7 and a more robust effect of PIF3 was observed, a situation that was reversed in *XTR7*, where the contribution of PIF7 was more prominent (Fig. 5B). In both cases, small additive effects between both PIFs were observed. For *HFR1*, the contributions of PIF3 and PIF7 were more similar, and no additive effects were observed. These results were somewhat surprising considering the prominent role of PIF7 in

promoting growth at least under EODFR conditions (Fig. 4C), and in inducing some of these genes like *PIL1* in response to shade (Li et al. 2012), and suggested that under short day PIF7 might preferentially target a different set of genes. Therefore we extended this analysis by screening the list of shade-induced PIF7-dependent genes (Li et al. 2012), and identified two candidate genes, the transcription factor *HAT2* (*AT5G47370*) and the protein phosphatase 2C *MIDA9* (*AT5G02760*), which regulate different facets of photomorphogenesis (Sentandreu et al. 2011, 2012, Bou-Torrent et al. 2012) and show a diurnal pattern of expression under SDs similar to *PIL1*, *HFR1* and *XTR7* (http://diurnal.mocklerlab.org). In agreement, our data showed that under SDs (Fig. 5A), expression of *HAT2* and *MIDA9* increased towards the end of the night in WT seedlings (ZT24; D24) and decreased upon 1h illumination in the next day (ZT25; W25). Expression analysis showed that the expression levels were strongly attenuated at the end of the night in *pif7* mutants, with minor to absent effects in the *pif3* mutant (Fig. 5A), in sharp contrast to *PIL1*, *HFR1* and *XTR7*. Under SD-EODFR conditions, the rapid and transient induction of *HAT2* and *MIDA9* was also strongly dependent on PIF7, whereas the *pif3* mutant was unaffected (Fig. 5B). Whereas the *pif3pif7* mutant was indistinguishable from *pif7* mutants under SD, in SD-EODFR small additive or synergistic effects were observed at least for *MIDA9*. Together, these data suggest that the molecular phenotype in SD and SD-EODFR is established by complex functional interactions between PIF3 and PIF7 that vary from gene to gene. Some of these combinatorial activities between PIF3 and PIF7, especially under EODFR conditions, might involve the formation of heterodimers as shown above (Figure 3). Previous data have indicated that PIF3 accumulates progressively along the night to peak at dawn (Soy et al. 2012). phyB activity keeps PIF3 levels low at the beginning of the night, and inactivation of phyB by an EOD-FR induces higher PIF3 accumulation (Soy et al. 2012, 2014).

PIF7 protein mobility fluctuates in response to SD and SD-EODFR

It has been previously reported that the *PIF7* transcript oscillates under diurnal conditions in adult plants (Lee and Thomashow 2012) and in free running conditions (Kidokoro et al. 2009). In agreement with these reports, we also observed that *PIF7* transcript oscillates in young seedlings growing under diurnal short day (SD) conditions (Fig. 6A). In addition, it is well known that phy induces the accumulation of an inactive PIF7 phosphorylated form in high R/FR that presents a reduced mobility compared to the dephosphorylated form (Li et al. 2012). These studies show that the PIF7-phosphorylated form accumulates in light, but it dephosphorylates rapidly in response to shade, and this activated form of PIF7 accumulates in the nucleus to induce gene expression (Huang et al. 2018). Here we use the PIF7-flash lines (Li et al. 2012) to study accumulation of PIF7 in SD and in SD-EODFR. At the end of the light period in SD (W8) we observed a band with lower mobility, consistent with the described inactive phosphorylated form (Fig. 6B and 6C). In contrast, during the night, the fast migrating band (the active

dephosphorylated form) accumulates with a major peak (Niwa et al. 2009) at D24 compared to D9 (Fig. 6B). Results are consistent with gradual accumulation of the dephosphorylated form during the night under SD (Jiang et al. 2019). We also observe a rapid appearance of the slow migrating band upon switching lights on at ZT1 of the following day (W1) (Fig. 6B). In contrast, in response to EODFR, we observe a rapid complete disappearance of the slow migrating band at ZT9 (FR9) compared to SD (D9) (Fig. 6C). This EOD-FR pulse did not affect the overall pattern of accumulation of the *PIF7* transcript along the night, although levels were somewhat reduced compared to SD (Fig. 6A), in accordance to previous reports (Mizuno et al. 2015). These results suggest that inactivation of phyB by EODFR rapidly decreases the accumulation of the inactive phosphorylated form of PIF7 to induce growth under these conditions.

DISCUSSION

Previously, using a combination of SD and SD-EODFR light regimes, we reported the concerted action of PIF1, PIF3, PIF4, and PIF5 (the PIF quartet or PIFq) in promoting and optimizing hypocotyl elongation in diurnal conditions (Soy et al. 2014). However, because the *pifq* mutant still retained some responsiveness to SD-EODFR, participation of additional factors was suggested. The experiments presented here examine the contribution of PIF7 to seedling growth under diurnal conditions. In response to the long nights of SD photoperiods, PIF7 induces growth together with PIF3 and other PIFq members, whereas PIF7 activity is suppressed by phyB in constant WL or LD. Using a combination of LD, LD-EODFR, SD, and SD-EODFR experiments (Fig. 1A) in higher-order mutant seedlings lacking up to five PIFs, our data indicate that PIF7 is a prominent target of phyB-mediated suppression of growth under diurnal conditions. Furthermore, we establish that the growth-promotion activity of PIF7 together with the PIFq is likely sufficient to explain the photoperiodic control of seasonal growth in Arabidopsis. Finally, we show that diurnal oscillation of PIF7 activity involves increased activation by dephosphorylation during the dark hours. Consistent with these findings, our EODFR experiments establish that residual phy Pfr inhibits full activation of PIF7 during the long nights of SD.

The phenotypic and marker gene expression analysis of *pif7* single and higher order mutants presented here identify PIF7 as an additional PIF factor promoting growth under diurnal conditions through regulation of growth-related gene expression. PIFq function is antagonistic to the growth suppressing activity of phyB, which targets the PIFq for degradation, not only during the day but also during early night due to the relatively slow Pfr-to-Pr dark reversion rate (Soy et al. 2012, 2014, Sweere et al. 2001, Rausenberger et al. 2010), effectively suppressing growth in non-inductive conditions of LD (Fig. 1 and 2; (Niwa et al. 2009)). Consistently, a phy-inactivating EODFR pulse before the beginning of the 16 h night period in SDs was shown to promote accumulation of PIF3 and possibly other PIF proteins (Soy et al. 2014, Shen et al. 2005), and to

enhance hypocotyl growth by 3-fold during the night period (Soy et al. 2014). Our observations here suggest that PIF7, similarly to PIFq, promotes growth in response to the long nights of SD (Fig. 1 and 2), also in antagonistic fashion toward phyB, as shown by the partial suppression of the *phyB* elongated phenotype in the *phyBpif7* mutant (Fig. 1). Interestingly, our observation that the contribution of PIF7 to growth is not as strong as PIF3 under SD, but that it appears to contribute more robustly than PIF3 under SD-EODFR (Fig. 2 and 4), suggests that inhibition of PIF7 by phyB during early night is central to suppression of growth under these conditions.

The observation that the apparent relative contribution of PIF7 and PIF3 to full induction of growth-related genes under SD varies among genes (Fig. 5) suggests that PIF7 and PIF3 have both shared and specific regulatory functions: whereas PIF3 dominates expression of *PIL1*, *HFR1*, and *XTR7*, PIF7 is a strong contributor to the induction of *HAT2* and *MIDA9*, with non-detectable to minor effects of PIF3 (Fig. 5A). In contrast to SD, examination of marker gene expression under SD-EODFR showed a robust increase with respect to SD in accordance to previous data (Soy et al. 2014), and revealed an enhanced relative contribution of PIF7 compared to PIF3 for some of the growth-related marker genes like *XTR7* (Fig. 5B). These results agree with the increased contribution of PIF7 function to hypocotyl growth under SD-EODFR compared to SD, and suggest that PIF7 role might be relatively more important in conditions where it has been suggested that seedlings experience a partial reversion to the etiolated state, like SD-EODFR (Soy et al. 2014) as shown in this work, or in shade-induced responses (Leivar et al. 2012b), where PIF7 plays a prominent role (Li et al. 2012, Mizuno et al. 2015, Jiang et al. 2019). Also in agreement, a recent paper reported that several shade-induced genes display remarkable divergence in dependency on the PIF quartet and PIF7 for their shade responsiveness, indicating a spectrum of combinatorial activities toward these genes (Zhang et al. 2020). Part of the observed functional interaction between PIF7 and PIFq could involve heterodimer formation, including the newly described PIF7-PIF3 heterodimers (Fig. 3).

The results presented here indicate that sequential removal of PIFs in *pif3pif4*, *pif3pif4pif7*, *pif3pif4pif5*, *pif3pif4pif5pif7*, *pifq* and *pifqpif7* mutants progressively decreased the sensitivity to longer night periods and the associated growth response (Fig. 2). Our striking finding that a *pifqpif7* mutant remains very short in all photoperiodic conditions examined, and is nearly insensitive for hypocotyl elongation to SD-EODFR treatment (Fig. 2), indicates that the collective action of PIF7 and the PIFq can account for the implementation of the phy-regulated control of growth under diurnal conditions, and strongly suggests that the collective contribution of these five PIFs is required for the photoperiodic-regulated seasonal acceleration of growth. A recent observation that the *pifqpif7* quintuple mutant is unresponsive to long term exposure to low R/FR (Zhang et al. 2020) is consistent with our results. Together these findings establish that the five PIF-quintet members (PIFs1, -3, -4, -5, and -7) are collectively fully responsible for

promoting hypocotyl cell elongation in response to environments where there is a fluctuation in Pr/Pfr phy forms such as shade and diurnal conditions.

Our observation that *PIF7* transcript oscillates in SD (Fig. 6A), suggests that *PIF7* transcription is probably regulated by the circadian clock. Indeed, Kidokoro et al. (Kidokoro et al. 2009) showed a similar *PIF7* oscillatory pattern under free running conditions, a hallmark of regulation by the clock. This is similar to *PIF4* and *PIF5*, which also oscillate in SD under clock regulation, but in contrast to *PIF1* and *PIF3*, which show relatively constant transcript levels across the day and night under SD. Despite these similarities with PIF4 and PIF5, regulation of PIF7 protein stability is unique compared to the PIFq members. Indeed, the rapid light-induced interaction of PIF7 with photoactivated phyB does not lead to robust degradation of PIF7 (Leivar et al. 2008a, Lee and Thomashow 2012, Li et al. 2012). Instead, it triggers accumulation of a cytosolic, phosphorylated form of PIF7 under constant white light, which is rapidly dephosphorylated and transported to the nucleus in response to phy inactivation, such as in FR-enriched shade environments (low R/FR conditions) (Li et al. 2012, Peng et al. 2018). This dephosphorylated PIF7 can bind to genomic target sites and to chromatin remodeling machinery to regulate the expression of its target genes (Li et al. 2012, Huang et al. 2018), and can be rapidly photoreversed to the phosphorylated form when returned to white light (Li et al. 2012). Our results here in alternating day/night conditions, extend these observations to show that phy imposes oscillation of PIF7 activity under SD (Fig. 6): during the day, phy Pfr triggers accumulation of the inactive phosphorylated form of PIF7, whereas in the night reversion to Pr favors accumulation of the dephosphorylated form, which is active in the induction of gene expression (Fig. 5) and in the promotion of hypocotyl elongation, consistent with recent findings (Jiang et al. 2019).

Collectively, the data presented here indicate that PIF7, together with the PIFq, promote acceleration of hypocotyl elongation in response to photoperiod shortening (i.e. longer nights). The present work suggests that phy-mediated regulation of PIFq stability and PIF7 activity is a central regulatory pathway in conferring day-length sensitivity, in order to ensure growth in the appropriate season. Interestingly, our finding that phytochrome mediates inhibition of growth under SD by suppressing PIF7 activity (as revealed by our EODFR treatments) could represent a safety mechanism to prevent overgrowth while retaining a significant capacity to integrate and respond to situations in SD where additional rapid elongation is needed. Such scenarios could include shading or an increase in temperature. Indeed, high temperature has been shown to trigger fast Pr to Pfr thermal reversion of phyB (Legris et al. 2016, Jung et al. 2016), raising the levels of active PIF7 and increasing PIF4 accumulation, the two main PIFs involved in thermomorphogenesis downstream of phyB (Koini et al. 2009, Franklin et al. 2011, Lee and Thomashow 2012, Fiorucci et al. 2019). Together, the phyB/PIF7 module might equip seedlings

growing under diurnal conditions with the capacity to rapidly optimize their growth to changes in light quality or temperature.

AUTHOR CONTRIBUTIONS

P.L., and E.M. conceived and designed the study. P.L., G.M., J.S., J.D-R, P.H.Q., and E.M., acquired, analyzed, and interpreted data. P.L., and E.M. wrote the manuscript.

ACKNOWLEDGEMENTS

We thank M. Cohn and C. Coates for early work on the project, and J. Chory, Ullas Pedmale and L. Li for PIF7-flash lines. This work was supported by Marie Curie International Reintegration Grant PIRG06-GA-2009-256420 and by funds from Universitat Ramon Llull/Obra Social la Caixa (2016-URL-Internac-019, 2018-LC-05 and 2018-URL-IR2nQ-019) to P.L., by NIH (5R01GM047475-24) and USDA ARS Current Research Information System (2030-21000-051-00D) grants to P.H.Q., and by grants from the Spanish ‘‘Ministerio de Economía y Competitividad’’ (MINECO) (BIO2012-31672 and BIO2015-68460-P), by FEDER / Ministerio de Ciencia, Innovación y Universidades – Agencia Estatal de Investigación (Project Reference BIO2015-68460-P) and from the CERCA Programme / Generalitat de Catalunya (Project References 2014-SGR-1406 and 2017SGR-718) to E.M. We acknowledge financial support by the CERCA programme/Generalitat de Catalunya and from MINECO through the ‘‘Severo Ochoa Programme for Centers of Excellence in R&D’’ 2016-2019 (SEV-2015-0533).

REFERENCES

Al-Sady B, Ni W, Kircher S, Schäfer E, Quail PH (2006) Photoactivated Phytochrome Induces Rapid PIF3 Phosphorylation Prior to Proteasome-Mediated Degradation. Mol Cell 23: 439–446

Arana MV, Marín-De La Rosa N, Maloof JN, Blázqueza MA, Alabadí D (2011) Circadian oscillation of gibberellin signaling in Arabidopsis. Proc Natl Acad Sci U S A 108: 9292–9297

Bauer D, Viczián A, Kircher S, Nobis T, Nitschke R, Kunkel T, Panigrahi KCS, Ádám É, Fejes E, Schäfer E, Nagy F (2004) Constitutive photomorphogenesis 1 and multiple photoreceptors control degradation of phytochrome interacting factor 3, a transcription factor required for light signaling in Arabidopsis. Plant Cell 16: 1433–1445

Bernardo-García S, de Lucas M, Martínez C, Espinosa-Ruiz A, Davière J-M, Prat S (2014) BR-dependent phosphorylation modulates PIF4 transcriptional activity and shapes diurnal hypocotyl growth. Genes Dev 28: 1681–1694

Bou-Torrent J, Salla-Martret M, Brandt R, Musielak T, Palauqui J-C, Martínez-García JF, Wenkel S (2012) ATHB4 and HAT3, two class II HD-ZIP transcription factors, control leaf development in Arabidopsis. Plant Signal Behav 7: 1–6

507 Bu Q, Castillon A, Chen F, Zhu L, Huq E (2011) Dimerization and blue light regulation of PIF1
508 interacting bHLH proteins in Arabidopsis. Plant Mol Biol 77: 501–511
509 Castillon A, Shen H, Huq E (2007) Phytochrome Interacting Factors: central players in
510 phytochrome-mediated light signaling networks. Trends Plant Sci 12: 514–521
511 Fairchild CD, Schumaker MA, Quail PH (2000) HFR1 encodes an atypical bHLH protein that
512 acts in phytochrome A signal transduction. Genes Dev 14: 2377–2391
513 Fiorucci AS, Costa Galvão V, Ince YÇ, Boccaccini A, Goyal A, Allenbach Petrolati L, Trevisan
514 M, Fankhauser C (2019) PHYTOCHROME INTERACTING FACTOR 7 is important for
515 early responses to elevated temperature in Arabidopsis seedlings. New Phytol: [Epub ahead
516 of print]
517 Franklin KA, Lee SH, Patel D, Kumar SV, Spartz AK, Gu C, Ye S, Yu P, Breen G, Cohen JD,
518 Wigge PA, Gray WM (2011) Phytochrome-Interacting Factor 4 (PIF4) regulates auxin
519 biosynthesis at high temperature. Proc Natl Acad Sci U S A 108: 20231–20235
520 Galvão VC, Fiorucci AS, Trevisan M, Franco-Zorilla JM, Goyal A, Schmid-Siegert E, Solano R,
521 Fankhauser C (2019) PIF transcription factors link a neighbor threat cue to accelerated
522 reproduction in Arabidopsis. Nat Commun 10: 4005
523 Gommers CMM, Monte E (2018) Seedling establishment: A dimmer switch-regulated process
524 between dark and light signaling. Plant Physiol 176: 1061–1074
525 Hornitschek P, Lorrain S, Zoete V, Michielin O, Fankhauser C (2009) Inhibition of the shade
526 avoidance response by formation of non-DNA binding bHLH heterodimers. EMBO
527 JournalEMBO J 28: 3893–3902
528 Huang X, Zhang Q, Jiang Y, Yang C, Wang Q, Li L (2018) Shade-induced nuclear localization
529 of PIF7 is regulated by phosphorylation and 14-3-3 proteins in arabidopsis. Elife 7: 1–17
530 Jiang Y, Yang C, Huang S, Xie F, Xu Y, Liu C, Li L (2019) The ELF3-PIF7 interaction mediates
531 the circadian gating of the shade response in Arabidopsis. Iscience 22: 288–298
532 Jung JH, Domijan M, Klose C, Biswas S, Ezer D, Gao M, Khattak AK, Box MS, Charoensawan
533 V, Cortijo S, Kumar M, Grant A, Locke JC, Schäfer E, Jaeger KE, Wigge PA (2016)
534 Phytochromes function as thermosensors in Arabidopsis. Science (80-) 354: 886–889
535 Khanna R, Huq E, Kikis EA, Al-Sady B, Lanzatella C, Quail PH (2004) A novel molecular
536 recognition motif necessary for targeting photoactivated phytochrome signaling to specific
537 basic helix-loop-helix transcription factors. Plant Cell 16: 3033–3044
538 Kidokoro S, Maruyama K, Nakashima K, Imura Y, Narusaka Y, Shinwari ZK, Osakabe Y, Fujita
539 Y, Mizoi J, Shinozaki K, Yamaguchi-Shinozaki K (2009) The phytochrome-interacting
540 factor PIF7 negatively regulates dreb1 expression under circadian control in Arabidopsis.
541 Plant Physiol 151: 2046–2057
542 Koini MA, Alvey L, Allen T, Tilley CA, Harberd NP, Whitelam GC, Franklin KA (2009) High
543 Temperature-Mediated Adaptations in Plant Architecture Require the bHLH Transcription

544 Factor PIF4. Curr Biol 19: 408–413
545 Lee CM, Thomashow MF (2012) Photoperiodic regulation of the C-repeat binding factor (CBF)
546 cold acclimation pathway and freezing tolerance in Arabidopsis thaliana. Proc Natl Acad
547 Sci U S A 109: 15054–15059
548 Legris M, Klose C, Burgie ES, Costigliolo C, Neme M, Hiltbrunner A, Wigge PA, Schäfer E,
549 Vierstra RD, Casal JJ (2016) Phytochrome B integrates light and temperature signals in
550 Arabidopsis. Science (80-) 354: 897–900
551 Leivar P, Monte E (2014) PIFs: systems integrators in plant development. Plant Cell 26: 56–78
552 Leivar P, Monte E, Al-Sady B, Carle C, Storer A, Alonso JM, Ecker JR, Quail PH (2008a) The
553 Arabidopsis phytochrome-interacting factor PIF7, together with PIF3 and PIF4, regulates
554 responses to prolonged red light by modulating phyB levels. Plant Cell 20: 337–352
555 Leivar P, Monte E, Cohn MM, Quail PH (2012a) Phytochrome signaling in green Arabidopsis
556 seedlings: impact assessment of a mutually negative phyB-PIF feedback loop. Mol Plant 5:
557 734–749
558 Leivar P, Monte E, Oka Y, Liu T, Carle C, Castillon A, Huq E, Quail PH (2008b) Multiple
559 Phytochrome-Interacting bHLH Transcription Factors Repress Premature Seedling
560 Photomorphogenesis in Darkness. Curr Biol 18: 1815–1823
561 Leivar P, Tepperman JM, Cohn MM, Monte E, Al-Sady B, Erickson E, Quail PH (2012b)
562 Dynamic antagonism between phytochromes and PIF family basic helix-loop-helix factors
563 induces selective reciprocal responses to light and shade in a rapidly responsive
564 transcriptional network in Arabidopsis. Plant Cell 24: 1398–1419
565 Leivar P, Tepperman JM, Monte E, Calderon RH, Liu TL, Quail PH (2009) Definition of early
566 transcriptional circuitry involved in light-induced reversal of PIF-imposed repression of
567 photomorphogenesis in young Arabidopsis seedlings. Plant Cell 21: 3535–3553
568 Li L, Ljung K, Breton G, Schmitz RJ, Pruneda-Paz J, Cowing-Zitron C, Cole BJ, Ivans LJ,
569 Pedmale UV, Jung HS, Ecker JR, Kay SA, Chory J (2012) Linking photoreceptor excitation
570 to changes in plant architecture. Genes Dev 26: 785–790
571 Martín G, Rovira A, Veciana N, Soy J, Toledo-Ortiz G, Gommers CMM, Boix M, Henriques R,
572 Minguet EG, Alabadí D, Halliday KJ, Leivar P, Monte E (2018) Circadian Waves of
573 Transcriptional Repression Shape PIF-Regulated Photoperiod-Responsive Growth in
574 Arabidopsis. Curr Biol 28: 311-318.e5
575 Martínez-García JF, Huq E, Quail PH (2000) Direct targeting of light signals to a promoter
576 element-bound transcription factor. Science (80-) 288: 859–863
577 Mizuno T, Oka H, Yoshimura F, Ishida K, Yamashino T (2015) Insight into the mechanism of
578 end-of-day far-red light (EODFR)-induced Shade avoidance responses in Arabidopsis
579 thaliana. Biosci Biotechnol Biochem 79: 1987–1994
580 Monte E, Alonso JM, Ecker JR, Zhang Y, Li X, Young J, Austin-Phillips S, Quail PH (2003)

581 Isolation and characterization of phyC mutants in Arabidopsis reveals complex crosstalk
582 between phytochrome signaling pathways. Plant Cell 15: 1962–1980
583 Monte E, Tepperman JM, Al-Sady B, Kaczorowski KA, Alonso JM, Ecker JR, Li X, Zhang Y,
584 Quail PH (2004) The phytochrome-interacting transcription factor, PIF3, acts early,
585 selectively, and positively in light-induced chloroplast development. Proc Natl Acad Sci U
586 S A 101: 16091–16098
587 Ni M, Tepperman JM, Quail PH (1999) Binding of phytochrome B to its nuclear signalling
588 partner PIF3 is reversibly induced by light. Nature 400: 781–784
589 Ni M, Tepperman JM, Quail PH (1998) PIF3, a phytochrome-interacting factor necessary for
590 normal photoinduced signal transduction, is a novel basic helix-loop-helix protein. Cell 95:
591 657–667
592 Nieto C, López-Salmerón V, Davière JM, Prat S (2015) ELF3-PIF4 interaction regulates plant
593 growth independently of the evening complex. Curr Biol 25: 187–193
594 Niwa Y, Yamashino T, Mizuno T (2009) The circadian clock regulates the photoperiodic
595 response of hypocotyl elongation through a coincidence mechanism in arabidopsis thaliana.
596 Plant Cell Physiol 50: 838–854
597 Nohales MA, Liu W, Duffy T, Nozue K, Sawa M, Pruneda-Paz JL, Maloof JN, Jacobsen SE, Kay
598 SA (2019) Multi-level Modulation of Light Signaling by GIGANTEA Regulates Both the
599 Output and Pace of the Circadian Clock. Dev Cell 49: 840-851.e8
600 Nomoto Y, Kubozono S, Yamashino T, Nakamichi N, Mizuno T (2012) Circadian clock-and
601 PIF4-controlled plant growth: A coincidence mechanism directly integrates a hormone
602 signaling network into the photoperiodic control of plant architectures in arabidopsis
603 thaliana. Plant Cell Physiol 53: 1950–1964
604 Nozue K, Covington MF, Duek PD, Lorrain S, Fankhauser C, Harmer SL, Maloof JN (2007)
605 Rhythmic growth explained by coincidence between internal and external cues. Nature 448:
606 358–361
607 Nozue K, Harmer SL, Maloof JN (2011) Genomic analysis of circadian clock-, light-,and growth-
608 correlated genes reveals PHYTOCHROME-INTERACTING FACTOR5 as a modulator of
609 auxin signaling in arabidopsis. Plant Physiol 156: 357–372
610 Nusinow DA, Helfer A, Hamilton EE, King JJ, Imaizumi T, Schultz TF, Farré EM, Kay SA
611 (2011) The ELF4-ELF3-LUX complex links the circadian clock to diurnal control of
612 hypocotyl growth. Nature 475: 398–404
613 Oh E, Zhu JY, Wang Z-Y (2012) Interaction between BZR1 and PIF4 integrates brassinosteroid
614 and environmental responses. Nat Cell Biol 14: 802–809
615 Park E, Kim Y, Choi G (2018) Phytochrome B requires PIF degradation and sequestration to
616 induce light responses across a wide range of light conditions. Plant Cell 30: 1277–1292
617 Peng M, Li Z, Zhou N, Ma M, Jiang Y, Dong A, Shen WH, Li L (2018) Linking phytochrome-

618 interacting factor to histone modification in plant shade avoidance. Plant Physiol 176: 1341–
619 1351
620 Pham VN, Kathare PK, Huq E (2018) Phytochromes and phytochrome interacting factors. Plant
621 Physiol 176: 1025–1038
622 Rausenberger J, Hussong A, Kircher S, Kirchenbauer D, Timmer J, Nagy F, Schäfer E, Fleck C
623 (2010) An integrative model for phytochrome B mediated photomorphogenesis: From
624 protein dynamics to physiology. PLoS One 5: e10721
625 Reed JW, Nagpal P, Poole DS, Furuya M, Chory J (1993) Mutations in the gene for the red/far-
626 red light receptor phytochrome B alter cell elongation and physiological responses
627 throughout arabidopsis development. Plant Cell 5: 147–157
628 Sentandreu M, Leivar P, Martín G, Monte E (2012) Branching of the PIF3 regulatory network in
629 Arabidopsis. Plant Signal Behav 7: 510–513
630 Sentandreu M, Martín G, González-Schain N, Leivar P, Soy J, Tepperman JM, Quail PH, Monte
631 E (2011) Functional profiling identifies genes involved in organ-specific branches of the
632 PIF3 regulatory network in Arabidopsis. Plant Cell 23: 3974–3991
633 Shen H, Moon J, Huq E (2005) PIF1 is regulated by light-mediated degradation through the
634 ubiquitin-26S proteasome pathway to optimize photomorphogenesis of seedlings in
635 Arabidopsis. Plant J 44: 1023–1035
636 Shen H, Zhu L, Castillon A, Majee M, Downie B, Huq E (2008) Light-induced phosphorylation
637 and degradation of the negative regulator phytochrome-interacting factor1 from Arabidopsis
638 depend upon its direct physical interactions with photoactivated phytochromes. Plant Cell
639 20: 1586–1602
640 Shen Y, Khanna R, Carle CM, Quail PH (2007) Phytochrome induces rapid PIF5 phosphorylation
641 and degradation in response to red-light activation. Plant Physiol 145: 1043–1051
642 Shin J, Park E, Choi G (2007) PIF3 regulates anthocyanin biosynthesis in an HY5-dependent
643 manner with both factors directly binding anthocyanin biosynthetic gene promoters in
644 Arabidopsis. Plant J 49: 981–994
645 Soy J, Leivar P, González-Schain N, Martín G, Diaz C, Sentandreu M, Al-Sady B, Quail PH,
646 Monte E (2016) Molecular convergence of clock and photosensory pathways through PIF3-
647 TOC1 interaction and co-occupancy of target promoters. Proc Natl Acad Sci U S A 113:
648 4870–4875
649 Soy J, Leivar P, González-Schain N, Sentandreu M, Prat S, Quail PH, Monte E (2012)
650 Phytochrome-imposed oscillations in PIF3 protein abundance regulate hypocotyl growth
651 under diurnal light/dark conditions in Arabidopsis. Plant J 71: 390–401
652 Soy J, Leivar P, Monte E (2014) PIF1 promotes phytochrome-regulated growth under
653 photoperiodic conditions in Arabidopsis together with PIF3, PIF4, and PIF5. J Exp Bot 65:
654 2925–2936

Sweere U, Eichenberg K, Lohrmann J, Mira-Rodado V, Bäurle I, Kudla J, Nagy F, Schäfer E, Harter K (2001) Interaction of the response regulator ARR4 with phytochrome B in modulating red light signaling. Science (80-) 294: 1108–1111

Toledo-ortiz G, Huq E, Quail PH (2003) The Arabidopsis basic/helix-loop-helix transcription factor family. Plant Cell 15: 1749–1770

de Wit M, Keuskamp DH, Bongers FJ, Hornitschek P, Gommers CMM, Reinen E, Martínez-Cerón C, Fankhauser C, Pierik R (2016) Integration of Phytochrome and Cryptochrome Signals Determines Plant Growth during Competition for Light. Curr Biol 26: 3320–3326

de Wit M, Ljung K, Fankhauser C (2015) Contrasting growth responses in lamina and petiole during neighbor detection depend on differential auxin responsiveness rather than different auxin levels. New Phytol 208: 198–209

Yamashino T, Nomoto Y, Lorrain S, Miyachi M, Ito S, Nakamichi N, Fankhauser C, Mizuno T (2013) Verification at the protein level of the pif4-mediated external coincidence model for the temperature-adaptive photoperiodic control of plant growth in Arabidopsis thaliana. Plant Signal Behav 8: e23390

Zhang R, Yang C, Jiang Y, Li L (2019) A PIF7-CONSTANS-Centered Molecular Regulatory Network Underlying Shade-Accelerated Flowering. Mol Plant 12: 1587–1597

Zhang Y, Pfeiffer A, Tepperman JM, Dalton-Roesler J, Leivar P, Gonzalez Grandio E, Quail PH (2020) Central clock components modulate plant shade avoidance by directly repressing transcriptional activation activity of PIF proteins. Proc Natl Acad Sci 117: 3261–3269

DATA AVAILABILITY STATEMENT

The data that support the findings of this study are available from the corresponding authors upon reasonable request.

FIGURE LEGENDS

Fig. 1. PIF7 induces growth under diurnal short day (SD) conditions in antagonistic manner with phyB.

(A) Schematic view of the treatments used. Seedlings were grown for 4 days under WL, long day (LD, 16hWL:8hD) and short day (SD, 8hWL:16hD) photoperiods, or under LD and SD conditions submitted to a phy-inactivating far red pulse at the end of the day (LD-EODFR and SD-EODFR).

(B) Visible phenotypes of 4d-old seedlings grown in SD or in constant white light (WL).

(C) Quantification of hypocotyl elongation of 4d-old seedlings grown under the indicated conditions. Data represent the mean and standard error of at least 25 seedlings. Letters denote statistically significant differences among means by the Tukey's test ($p < 0.05$). Independent tests were assayed for each experimental condition.

(D) Data shown in panel C represented as a growth difference among the indicated treatments.

Fig. 2. *pifqpif7* mutants are insensitive to the photoperiodic control of seasonal growth.

(A) Visible phenotypes of 4d-old seedlings grown in SD and SD-EODFR as detailed in Fig. 1A.

(B) Quantification of hypocotyl elongation of 4d-old seedlings grown under the indicated conditions. Data represent the mean and standard error of at least 25 seedlings. Letters denote statistically significant differences among means by the Tukey's test ($p < 0.05$). Independent tests were assayed for each experimental condition.

(C) Data shown in panel B represented as a growth difference among the indicated treatments.

(D) Visible phenotypes of 4d-old seedlings grown in WL, SD and SD-EODFR.

Fig. 3. PIF7 is able to heterodimerize with PIF3.

A) PIF7 and PIF3 interact in vitro. Coimmunoprecipitation assays using GAL4 Activating Domain (GAD) alone or fused to full-length PIF7 (GAD:PIF7) and PIF3 (GAD:PIF3) as baits, while PIF7 was used as prey. Schematic diagrams on the top show the design of the experiment, and the SDS-PAGE separations of the pellet fractions and the inputs (10%) are shown below. Quantification of the binding expressed as % of bound PIF7 in relation to the initial PIF7 input and normalized to the bait used is shown at the bottom.

(B) PIF7 and PIF3 interact in a yeast two-hybrid assay. GAD, GAD:PIF3 and GAL4 DNA Binding domain (GBD) alone or fused to full length PIF7 (GBD:PIF7) were used for yeast two-hybrid interaction assays. Growth assays using restrictive media –LWA (top row) and –LWH (second row from top) were done to test for interaction in the yeast strain AH109. The control using non-restrictive –LW medium is shown in the third row. Interaction assay using qualitative β-galactosidase assay using Y187 yeast strain on plate is shown in the bottom row. The lower panel shows Miller units in a quantitative liquid β-galactosidase assay.

(C) PIF7 and PIF3 bind to the G-box DNA motif as heterodimer. Electrophoresis mobility shift assay (EMSA) showing TnT-translated PIF7 and GAD:PIF3 binding to the G-box as homodimers (lanes 4 and 3 respectively) and as a heterodimer (intermediate band in lane 5). TnT-only reactions were included as controls (lanes 2 and 6). FP= free probe. Lane 1 corresponds to FP-only binding reaction, and the asterisks indicate non-specific bands in the TnT-only reactions.

Fig. 4. Developmental and temporal regulation of hypocotyl growth by PIF3 and PIF7 under diurnal conditions.

(A) Quantification of hypocotyl elongation of seedlings grown for 2, 3 and 4 days in SD or in SD-EODFR. Letters denote statistically significant differences among means by the Tukey's test ($p < 0.05$) in SD (letters below lines) and SD-EODFR (letters above lines). Independent tests were assayed for each day and condition.

(B) Quantification of hypocotyl elongation of seedlings that were first grown for 2 days in WL (2d-WL) and then grown for 4 additional days in either WL, SD or SD-EODFR.

(C) Quantification of hypocotyl growth during the night hours of the 3rd day in SD or in SD-EODFR. Seedlings were grown for 2 days in SD (ZT0), and images of the seedlings were taken at the end of the day (ZT8, W8), and at the end of the night (ZT24) with (FR24) or without (D24) an EODFR pulse as indicated in the left panel. Hypocotyl length was measured (middle panel) and data were represented as a growth difference among the indicated time points (right panel). Data in A, B and C represent the mean and standard error of at least 25 seedlings. Letters denote statistically significant differences among means by the Tukey's test ($p < 0.05$). Independent tests were assayed for each experimental condition.

Fig. 5. PIF7, together with PIF3, acts to induce growth-related gene expression at night.

Gene expression was measured during the night hours of the 3rd day in SD (A) or in SD-EODFR (B). Seedlings were grown for 2 days in SD (ZT0) as in Fig. 4C, and samples were harvested at the at the end of the third day (ZT8, W8), and during the night hours at ZT9, ZT12, ZT16, ZT20 and ZT24 in seedlings treated with (FR9, FR12, FR16, FR20, FR24; panel B) or without (D9, D12, D16, D20, D24; panel A) an EODFR. An additional sample was harvested upon 1h illumination (ZT25, W25) during the 4th day of growth in SD (panel A). *PIL1*, *HFR1*, *XTR7*, *HAT2* and *MIDA9* expression relative to *PP2A* was measured and data are normalized to WT_D24 set at one. Data represent the mean and standard deviation of technical triplicates of one biological replicate.

Fig. 6. PhyB prevents full de-phosphorylation of PIF7 at night.

(A) PIF7 time-course expression in WT seedlings grown under SD or SD-EODFR. Seedlings were grown in SD. During the third day of growth, samples were either harvested at the indicated times (SD), or given an EODFR pulse and collected during the night at the indicated time points (SD-EODFR samples). PIF7 expression relative to PP2A was measured and normalized to the 0 time point (ZT0) set at one. Values are means of technical triplicates of one biological replicate.

(B) PIF7 protein level in SD at ZT8 (W8), ZT9 (D9), ZT24 (D24) and at 1h of the following day after illumination (W1).

(C) PIF7 protein level in SD-EODFR compared to SD at ZT8 (W8), ZT9 (FR9, D9) and at ZT24 (FR24, D24).

(B, C) Ponceau staining was used as a loading control. Blots correspond to one biological replicate.

Fig. 1

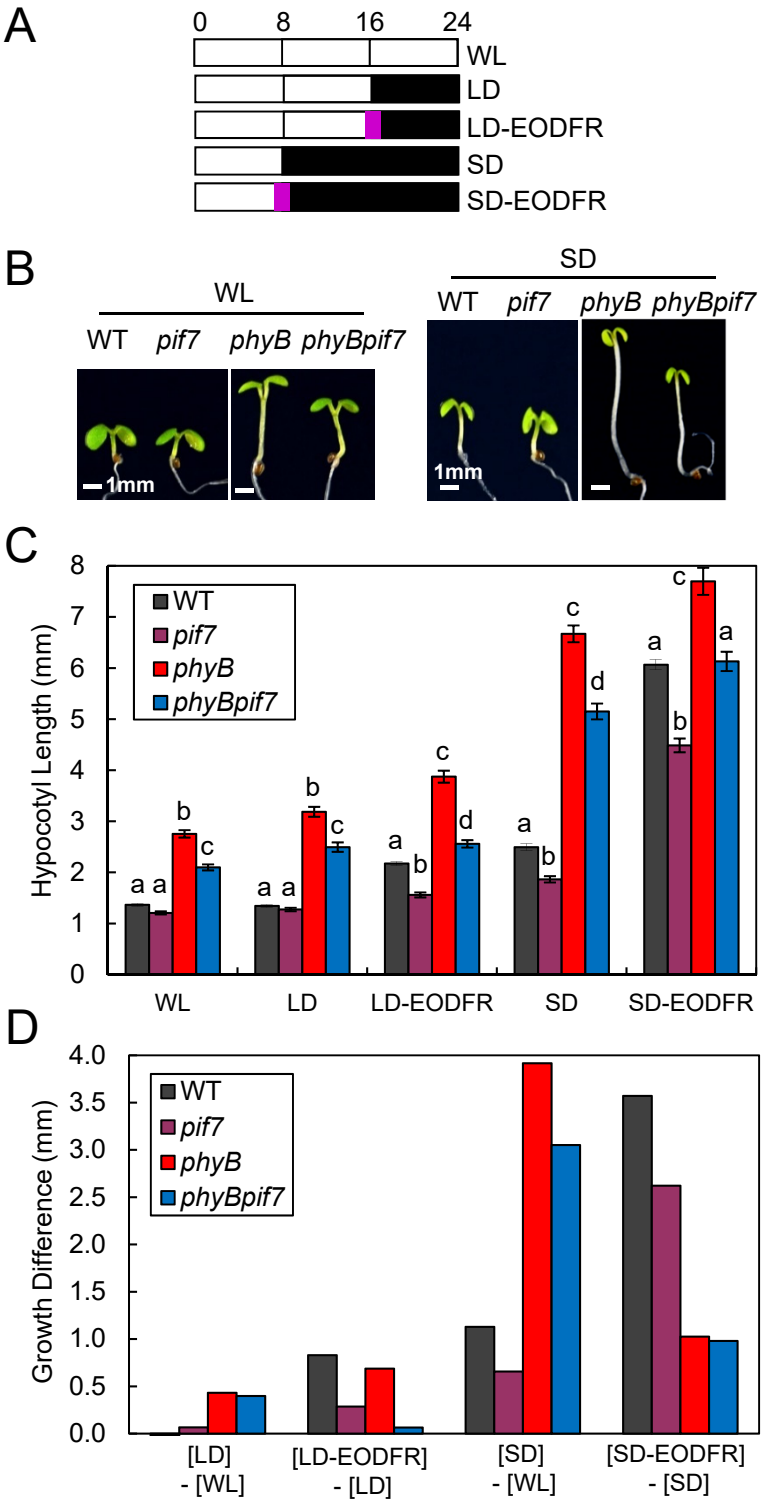
A
0
8
16
24
WL
LD
LD-EODFR
SD
SD-EODFR
B
WL
SD
WT
pif7
phyB
phyBpif7
1mm
C
Hypocotyl Length (mm)
WT
pif7
phyB
phyBpif7
WL
LD
LD-EODFR
SD
SD-EODFR
D
Growth Difference (mm)
[LD] - [WL]
[LD-EODFR] - [LD]
[SD] - [WL]
[SD-EODFR] - [SD]

Fig. 2

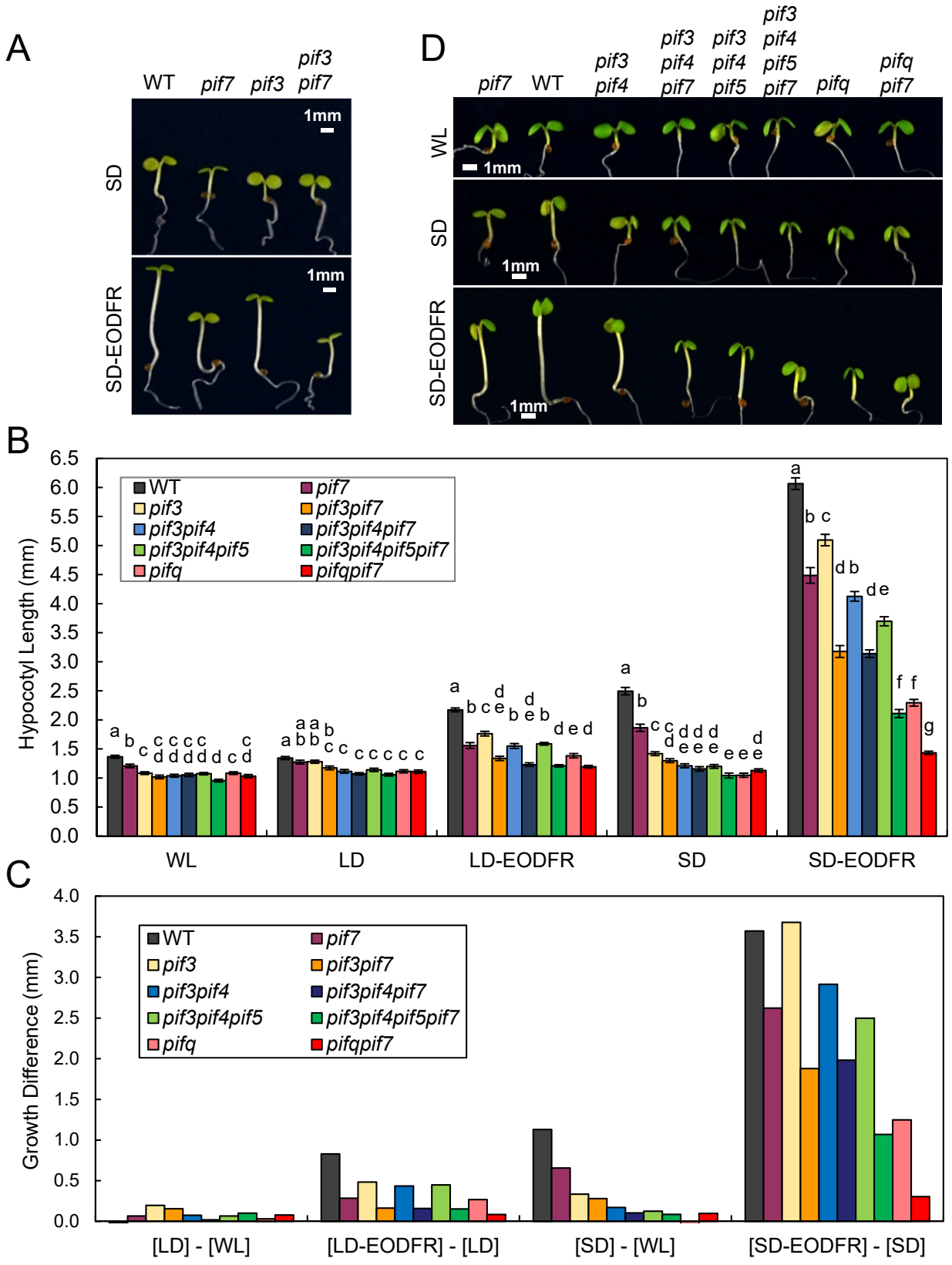
A
WT
pif7
pif3
pif3 pif7
SD
SD-EODFR
1mm
D
pif7
WT
pif3 pif4
pif3 pif4 pif7
pif3 pif4 pif5
pif3 pif4 pif5 pif7
pifq
pifq pif7
WL
SD
SD-EODFR
1mm
B
Hypocotyl Length (mm)
WT
pif7
pif3
pif3pif7
pif3pif4
pif3pif4pif7
pif3pif4pif5
pif3pif4pif5pif7
pifq
pifqpif7
WL
LD
LD-EODFR
SD
SD-EODFR
C
Growth Difference (mm)
[LD] - [WL]
[LD-EODFR] - [LD]
[SD] - [WL]
[SD-EODFR] - [SD]

Fig. 4

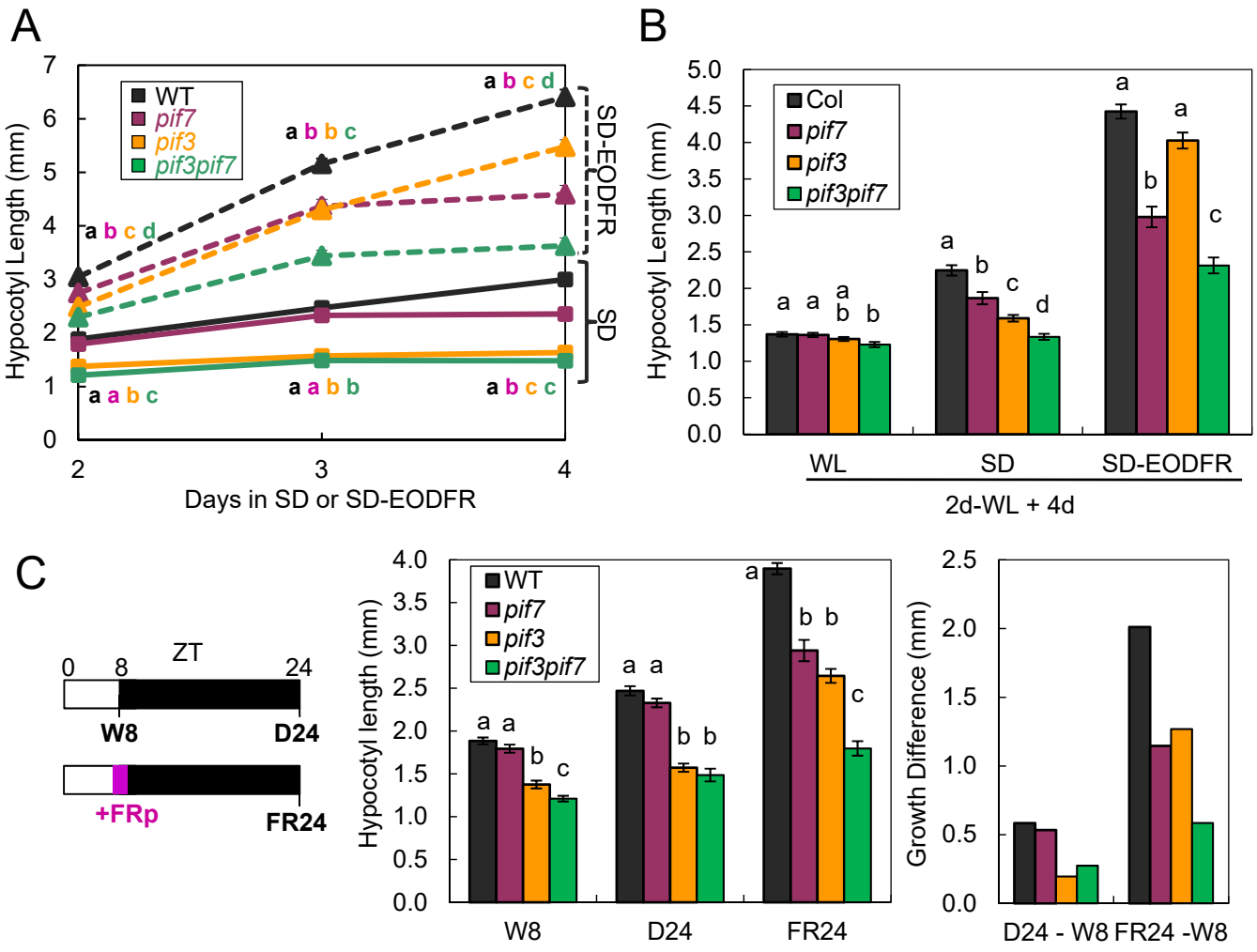
A
Hypocotyl Length (mm)
WT
pif7
pif3
pif3pif7
a b c d
a b b c
a a b c
a a b b
a b c c
SD-EODFR
SD
Days in SD or SD-EODFR
B
Hypocotyl Length (mm)
Col
pif7
pif3
pif3pif7
WL
SD
SD-EODFR
2d-WL + 4d
C
ZT
0
8
24
W8
D24
+FRp
FR24
Hypocotyl length (mm)
WT
pif7
pif3
pif3pif7
W8
D24
FR24
Growth Difference (mm)
D24 - W8
FR24 -W8

Fig. 5

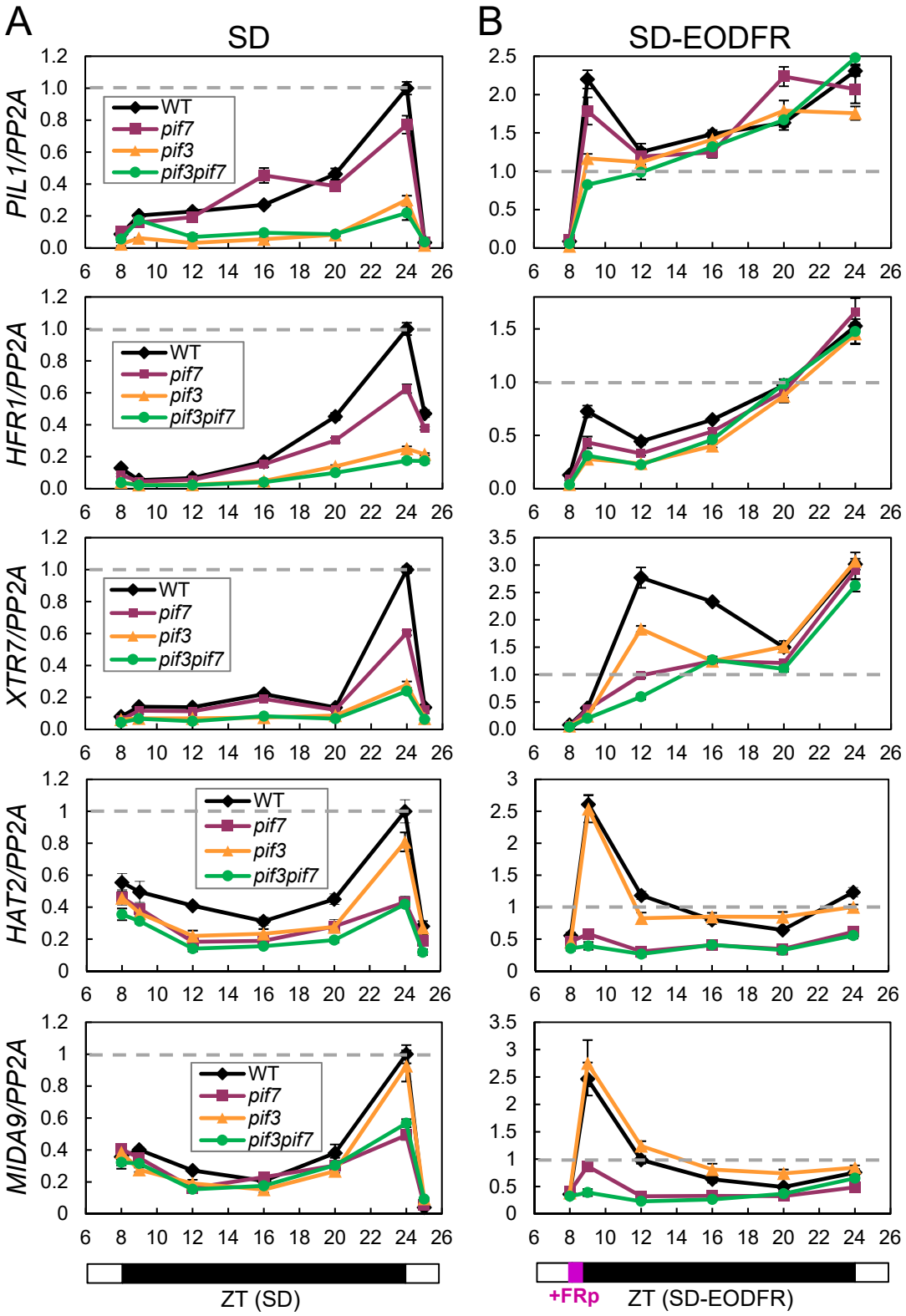
A
SD
B
SD-EODFR
PIL1/PP2A
HFR1/PP2A
XTR7/PP2A
HAT2/PP2A
MIDA9/PP2A
WT
pif7
pif3
pif3pif7
6 8 10 12 14 16 18 20 22 24 26
ZT (SD)
+FRp
ZT (SD-EODFR)

Fig. 6

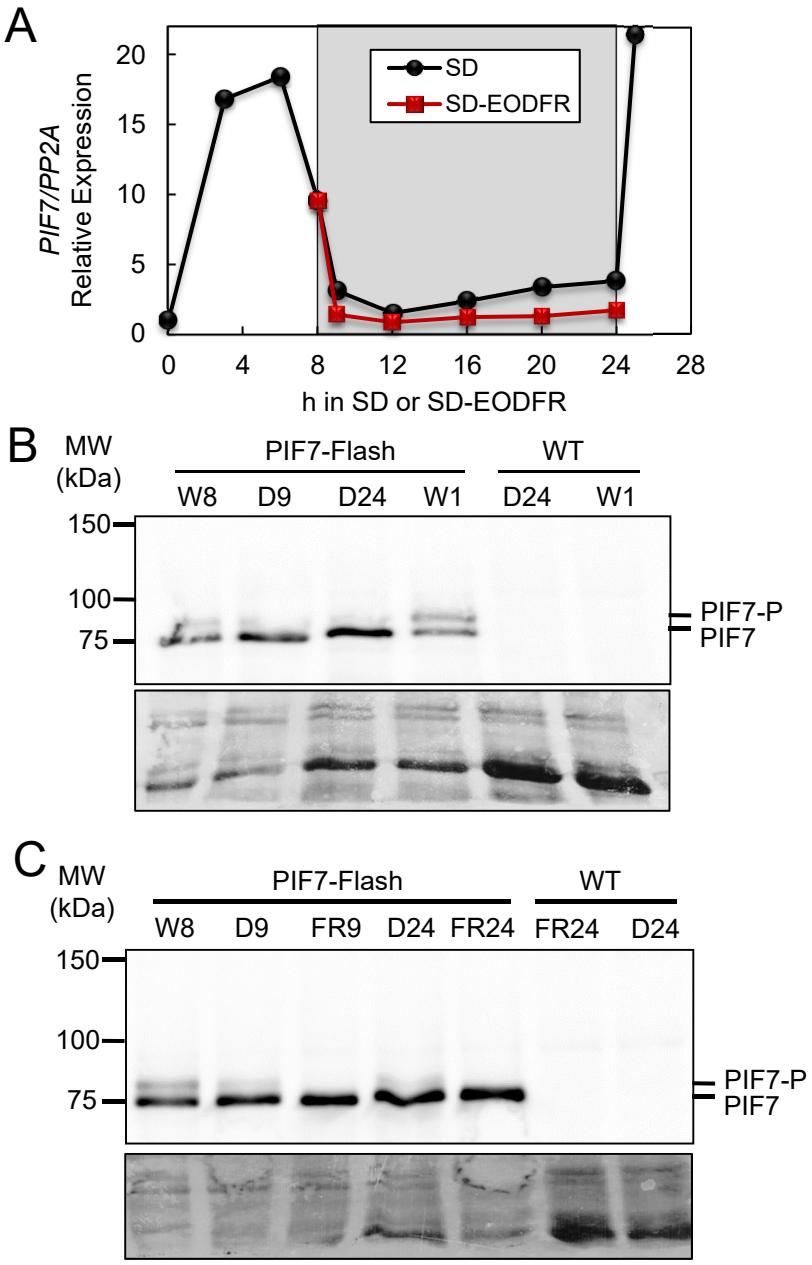
A
PIF7/PP2A
Relative Expression
20
15
10
5
0
SD
SD-EODFR
0
4
8
12
16
20
24
28
h in SD or SD-EODFR
B
MW
(kDa)
PIF7-Flash
WT
W8
D9
D24
W1
D24
W1
150
100
75
PIF7-P
PIF7
C
MW
(kDa)
PIF7-Flash
WT
W8
D9
FR9
D24
FR24
FR24
D24
150
100
75
PIF7-P
PIF7